Paleoceanography and Paleoclimatology

Supporting Information for

Seasonally Variable Aquifer Discharge and Cooler Climate in Bermuda during the Last Interglacial Revealed by Subannual Clumped Isotope Analysis

Jade Z. Zhang[1], Sierra V. Petersen[1], Ian Z. Winkelstern[2] and Kyger C Lohmann[1]

[1]Department of Earth and Environmental Science, University of Michigan, Ann Arbor, MI 48109, USA

[2]Department of Geology, Grand Valley State University, Allendale, MI 49401, USA

Contents of this file

Additional Supporting Information (Files uploaded separately)

Introduction

Extended text descriptions of the analytical methods including CO_2 preparation and Δ_{47} measurements, clumped isotope data processing, modern water preparation and isotope sampling, and salinity measurements. An annotated photo showing the isotope drilling locations and a diagram showing the custom-build vacuum extraction line. A plot showing all replicated salinity measurements for each water sample. A plot showing calculated modern shell temperature compared to modern observed temperature and precipitation. A version of the data calculated using Kim et al., 2007 aragonite-water equilibrium equation and Brand/IUPAC parameters with secondary transfer function. A plot showing modern observed temperature and annual tide. A plot showing tidal height verses water sample collection times and also a plot showing tidal height verses $\delta^{18}O_w$ values. A complete data table showing individual salinity and isotope measurement for each water sample has been uploaded separately.

Text S1. CO_2 Preparation and Δ_{47} Measurements

Seasonal peak and trough points were identified in the high resolution $\delta^{18}O$ data for each shell. Each identified $\delta^{18}O$ maximum or minimum was then sampled using a low speed dental drill until a total of 20 mg was collected and homogenized (Figure 3). Approximately 4-6 mg of powder was digested for 15-20 minutes in a common acid bath at a temperature of 75°C using 105 wt. % phosphoric acid (H_3PO_4). Extracted CO_2 was dehydrated through cryogenic separation at -95°C using a mixture of 1-propanol and liquid Nitrogen (LN_2) to remove any water generated during reaction. Dry CO_2 was then purified further by passing through a U-trap filled with PoraPak Q material and topped with silver wool to remove sulfur, chlorine, and other contaminants. Yields were recorded before and after this step using an electric manometer to ensure total sample recovery after the cleaning process. Lastly, purified CO_2 was transferred to a cold finger for temporary storage until analysis on the mass spectrometer was possible. All samples were replicated using the above procedure at least three times, with many samples replicated four times, spread out over a period of months to accommodate for long-term variation in mass spectrometer behavior.

Purified CO_2 was analyzed using a Thermo-Finnigan MAT 253 dual inlet mass spectrometer that has been specially configured to collect masses 44-49 against a reference gas with a composition of $\delta^{13}C$ = -3.69‰ (VPDB) and $\delta^{18}O$ = +34.98‰ (VSMOW). Both bellows were initially compressed to achieve 16 volts on the *m/z* 44 cup. Sample beam intensity for *m/z* 44-49 was measured against reference CO_2 beam intensity for 5 acquisitions of 12 sample-reference cycles for each purified CO_2 sample. All samples were replicated at least three times, with many samples replicated four times, spread out over a period of months to account for long-term variation in mass spectrometer behavior.

Text S2. Clumped Isotope Data Processing

In order to calculate Δ_{47} from raw mass spectrometer outputs (raw voltages), the absolute abundance of the heavy isotopes in the universal standards (VPDB, VSMOW) needs to be defined first using four parameters: R13_VPDB, R17_VSMOW, R18_VSMOW and λ (Petersen et al., 2019). These values were previously set and established by Santrock and coauthors (Santrock et al., 1985) but have been updated

recently (now known as Brand or IUPAC parameters) following improved measurement of the universal standard materials (Brand et al., 2010). Recent studies suggest that use of Brand parameters improves inter-laboratory agreement in clumped isotope calibrations and thus improves the accuracy of Δ_{47} data overall (Kelson et al., 2017; Petersen et al., 2019), making their use desirable and encouraged for all future studies.

Δ_{47} was calculated from raw voltages using an in-house R-code script applying the updated Brand parameters (Petersen et al., 2019). Δ_{47} values were converted into the absolute reference frame to correct the dependency of the measured Δ_{47} on δ_{47} and mass spectrometer "frame compression/stretching" using heated (1000^{o}C) and equilibrated (25^{o}C) gas standards (Dennis et al., 2011). An acid fractionation factor of +0.072‰ corresponding to a reaction temperature of 75°C was applied to account for the isotopic fractionation resulting from loss of one oxygen atom during acid digestion (Petersen et al., 2019). In-house carbonate standards (Carrara marble and aragonitic Ooids (Defliese et al 2015), and CORS coral standard (Rosenheim et al., 2013)) were monitored and correction windows were adjusted to minimize drift in corrected standard values through time. A secondary transfer function using Carrara, Ooids, CORS, and a handful of replicates of the ETH standards was applied, assigning the true values for in-house standards established independently relative to ETH standards. No secondary transfer function was applied to the Winkelstern et al. (2017) data due to insufficient standards run concurrently with samples during that period of time.

Individual replicates were determined to be bad if Δ_{48} values were elevated more than 2‰ above pure gas standards indicating contamination. Within each sample, if the standard deviation of the combined replicates was greatly in excess of the long-term standard deviation of in-house carbonate standards (0.025‰), the most deviant replicate was removed as an outlier, which in most cases corresponded to a single-replicate temperature of >50C or <-15C, likely representing individual errors during sample preparation. After this screening, only samples with at least 3 good replicates were included for interpretation. A complete version of the raw clumped isotope sample and standard replicates are provided separately.

Text S3. Modern Water Preparation and Isotope Analysis

All 17 seawater samples and 1 tapwater sample were analyzed for $\delta^{18}O$ in the University of Michigan Stable Isotope Laboratory. All aqueous samples were equilibrated with tank CO_2 before analysis on a Thermo-Finnegan MAT 253 dual inlet mass spectrometer. To prepare samples for equilibration, vials with sealed septa were first pierced with a needle and flushed and filled with dry tank CO_2 to a head-space pressure of 1 atm. 4 ml of an unknown or standard water was injected into each CO_2-containing vial, then left to equilibrate in a 25°C water bath for at least 48 hours. After the equilibration period, pure CO_2 was extracted on a custom-built vacuum extraction line (Figure S3). After all atmosphere remaining above frozen CO_2 was evacuated from the head space, CO_2 was cryogenically drawn out of the sample vial via a needle, then dehydrated through repeated stages of cryogenic separation at -95°C, achieved through a mixture of 1-propanol and liquid Nitrogen (LN_2), to remove any remaining water carried through the extraction line from equilibration. At this stage, yield of gas was checked using an electric manometer before dividing each sample into 3-6 aliquots. Each aliquot of CO_2 was separately flame sealed into a Pyrex tube for storage until analysis on the mass spectrometer. At least two aliquots of the same sample were measured on the mass spectrometer spread out over weeks to accommodate variation in mass spectrometer behavior, and one aliquot was archived in case a third measurement was needed in the future.

The extracted CO_2 was then analyzed on the same Thermo-Finnigan MAT 253 dual inlet mass spectrometer used for clumped isotope analyses (see Text S3). Unknown CO_2 was measured for at least 2 acquisitions of 12 sample-reference cycles at an m/z 44 beam strength of 16V. All samples were calibrated against in-house liquid standards which, in turn, were cross-calibrated using USGS standards (USGS 45, 46).

Text S4. Salinity Measurements

Salinity was measured twice on each seawater sample using an Extech EC170 salinity meter and a third time using a Leica handheld Temperature Compensated Refractometer for cross-calibration. Each sample was measured spread out over multiple days with randomized order. Salinity meters were cleaned with DI water in between each

sample, and wiped dry followed by further drying with compressed air to ensure they were thoroughly dry before the next measurement. Extech EC170 salinity meter measures conductivity and reports salinity to 0.1 ppt. A seawater sample from Florida (not part of this study) was measured 10 times using the Extech EC170 salinity meter to test reproducibility. This resulted in a salinity of 33.2 ± 0.3 ppt (1sd). Leica handheld Temperature Compensated Refractometer measures the angle of refraction in order to determine concentration of aqueous solutions, and has a typical precision of 0.5 ppt. Offset between the two methods was 1.2 ppt, with the refractometer typically higher. Reported salinities in the main document represent the mean of all three measurements (combining two methods), since one method was not verified to be better than the other.

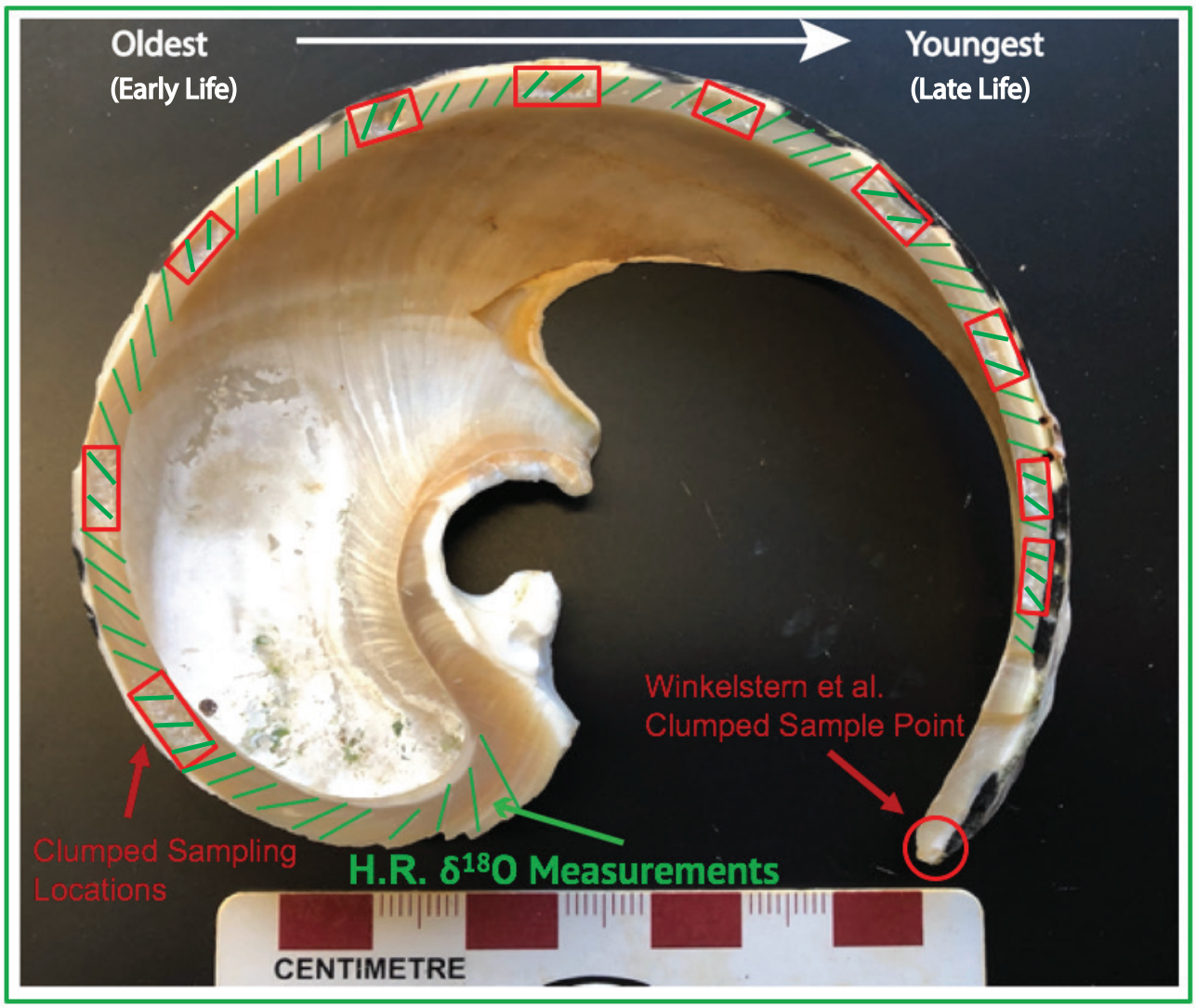

Figure S1. Annotated image of halved modern *C. pica* (BM2) with growth axis facing upwards. Representative high resolution $\delta^{18}O$ drill lines and larger clumped isotope sampling sites are highlighted in green and red, respectively.

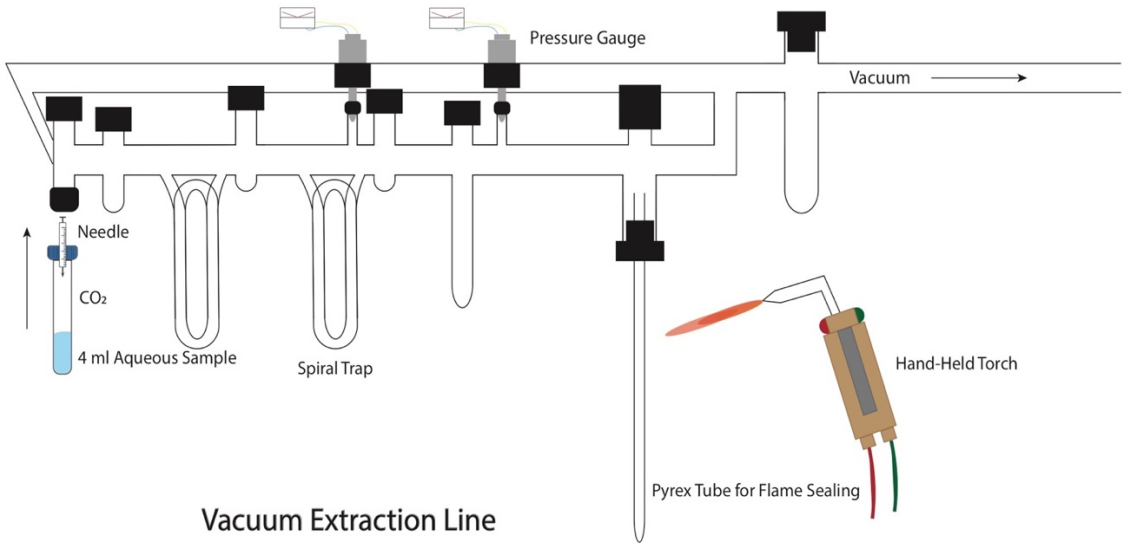

Figure S2. Diagram showing the custom-built vacuum extraction line. Note that the sample vial is introduced via a needle on the left side. Extracted CO_2 is then sealed in the pyrex tube on the right side.

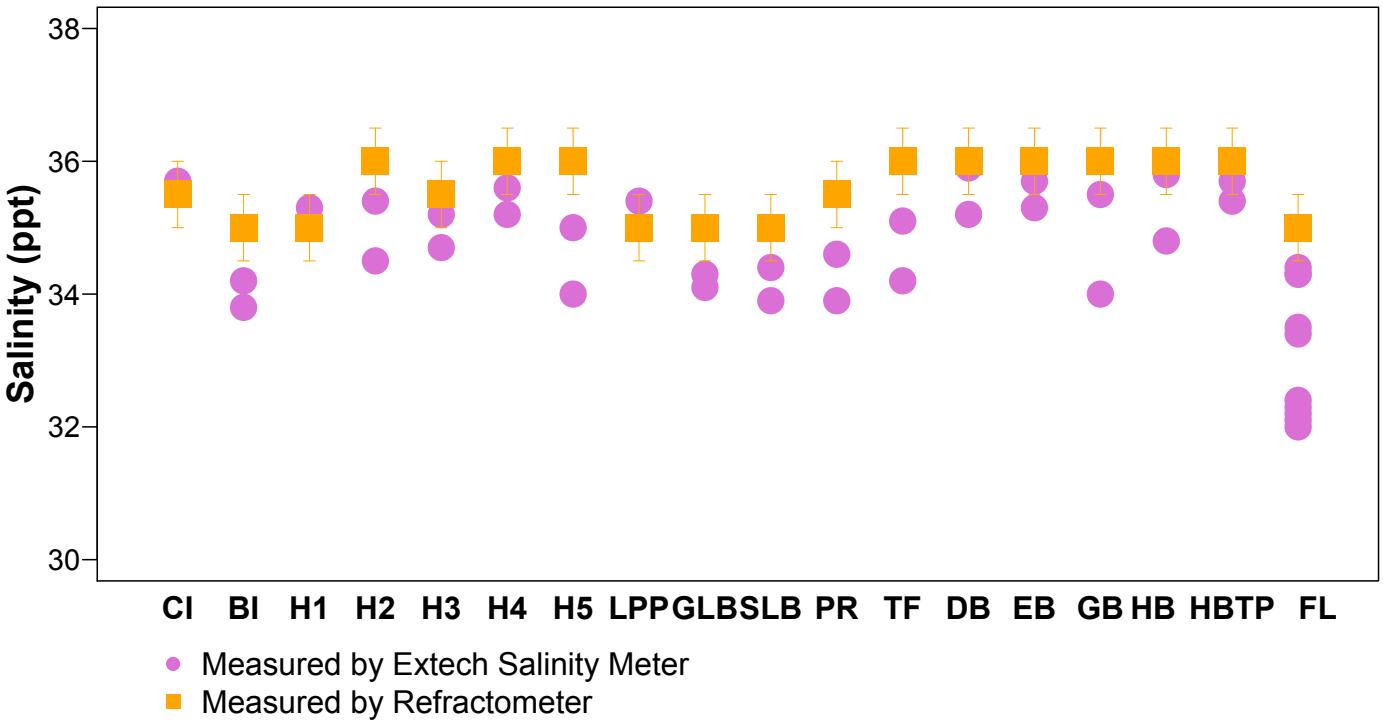

Figure S3. Salinity measurements for each modern water sample. Salinity was measured in duplicate using Extech EC170 salinity meter and a third time using the Leica handheld Temperature Compensated Refractometer. A randomly-selected sample (FL) was measured 10 times using the Extech EC170 salinity meter to test reproducibility.

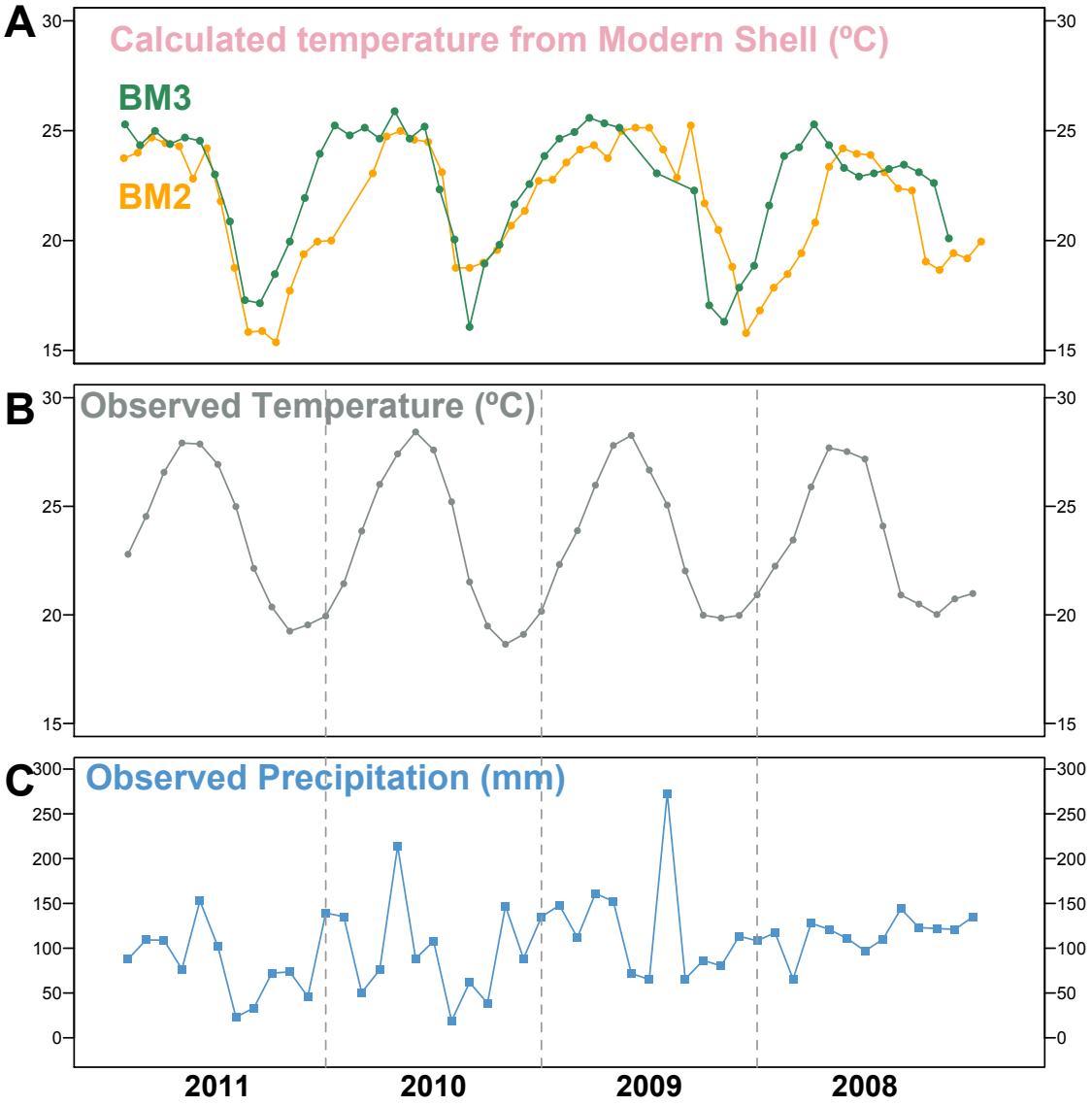

Figure S4. A, Calculated temperature, as was done in the original study, from high-resolution $\delta^{18}O_{carb}$ and a single $\delta^{18}O_w$ value of 1.16‰ ($\delta^{18}O_w$ value was selected from modern $\delta^{18}O_w$ measurement of the same site). X-axis is distance along growth axis, and has been stretched to roughly align with the temperature data in B. B, Observed modern (Instrumental) SST from 2008-2011 (NOAA National Data Buoy Center). C, Observed precipitation from 2008-2011 (LDEO Climate Group Datasets).

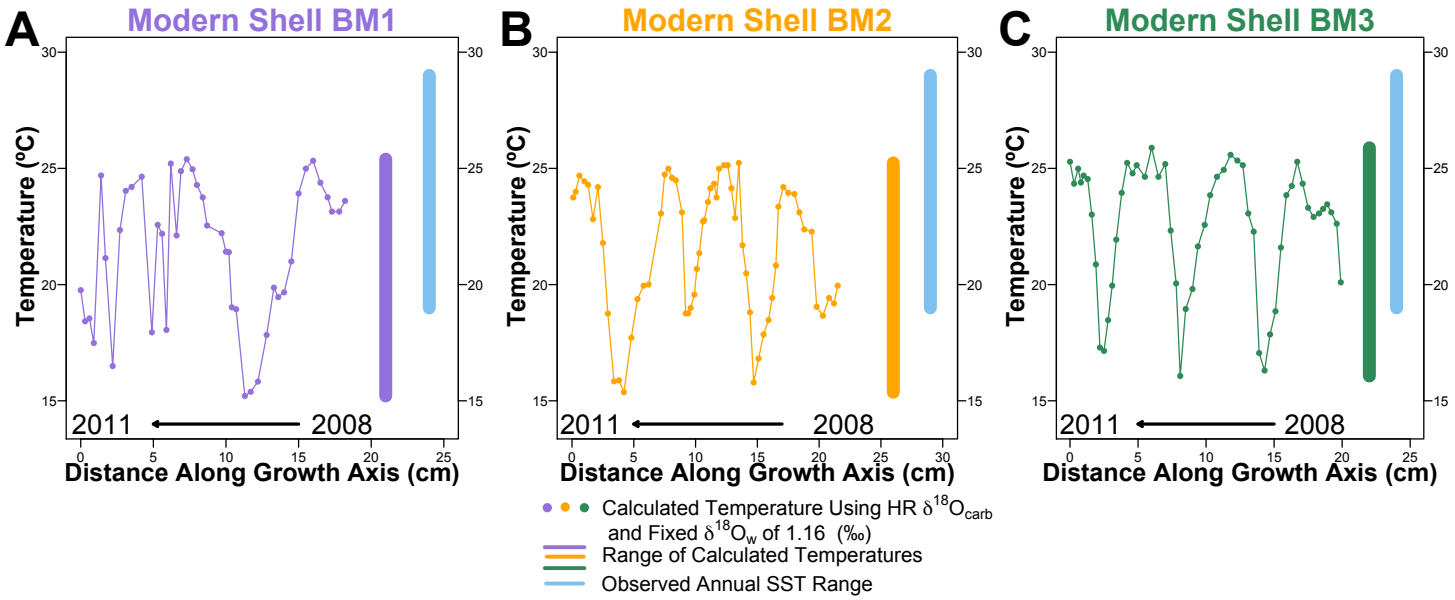

Figure S5. Temperature seasonality and range calculated for three modern shells (A. BM1, B. BM2, C. BM3), calculated from high-resolution $\delta^{18}O_{carb}$ profiles using a single $\delta^{18}O_w$ value of 1.16‰, selected from modern $\delta^{18}O_w$ measurement at collection site, and the water-aragonite fractionation factor of Kim et al. (2007). Blue bars show instrumental temperature range for comparison.

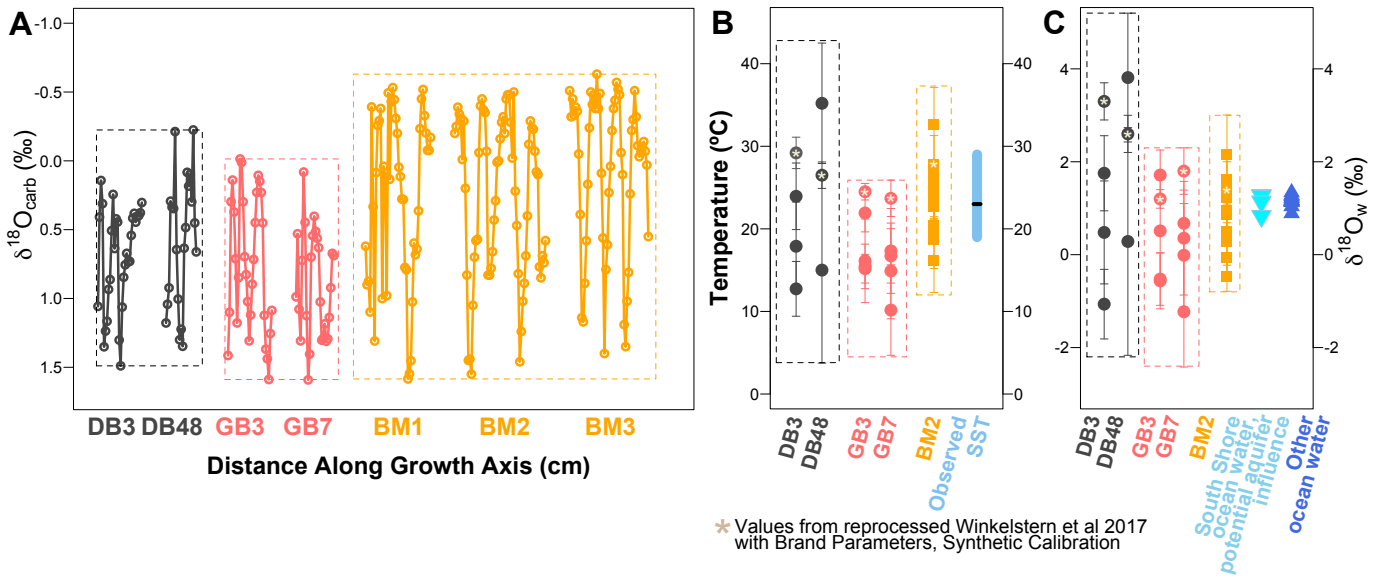

Figure S6. A, High Resolution $\delta^{18}O_{carb}$ ranges of fossil and modern shells. B, Temperature ranges of fossil and modern shells compared to modern SST on the right. Both DB/RB and GB show minimum temperatures colder than both modern shell and modern observations. C, $\delta^{18}O_w$ ranges of fossil and modern shells, calculated using Kim et al., 2007 aragonite-water equilibrium equation, compared to measured modern $\delta^{18}O_w$ values on the right. Both DB/RB and GB show a wider range in $\delta^{18}O_w$ than the modern shells due to their proximity to the central lens aquifer. Errors reported for both Δ_{47}-temperature and $\delta^{18}O_w$ values are based on 1 standard error.

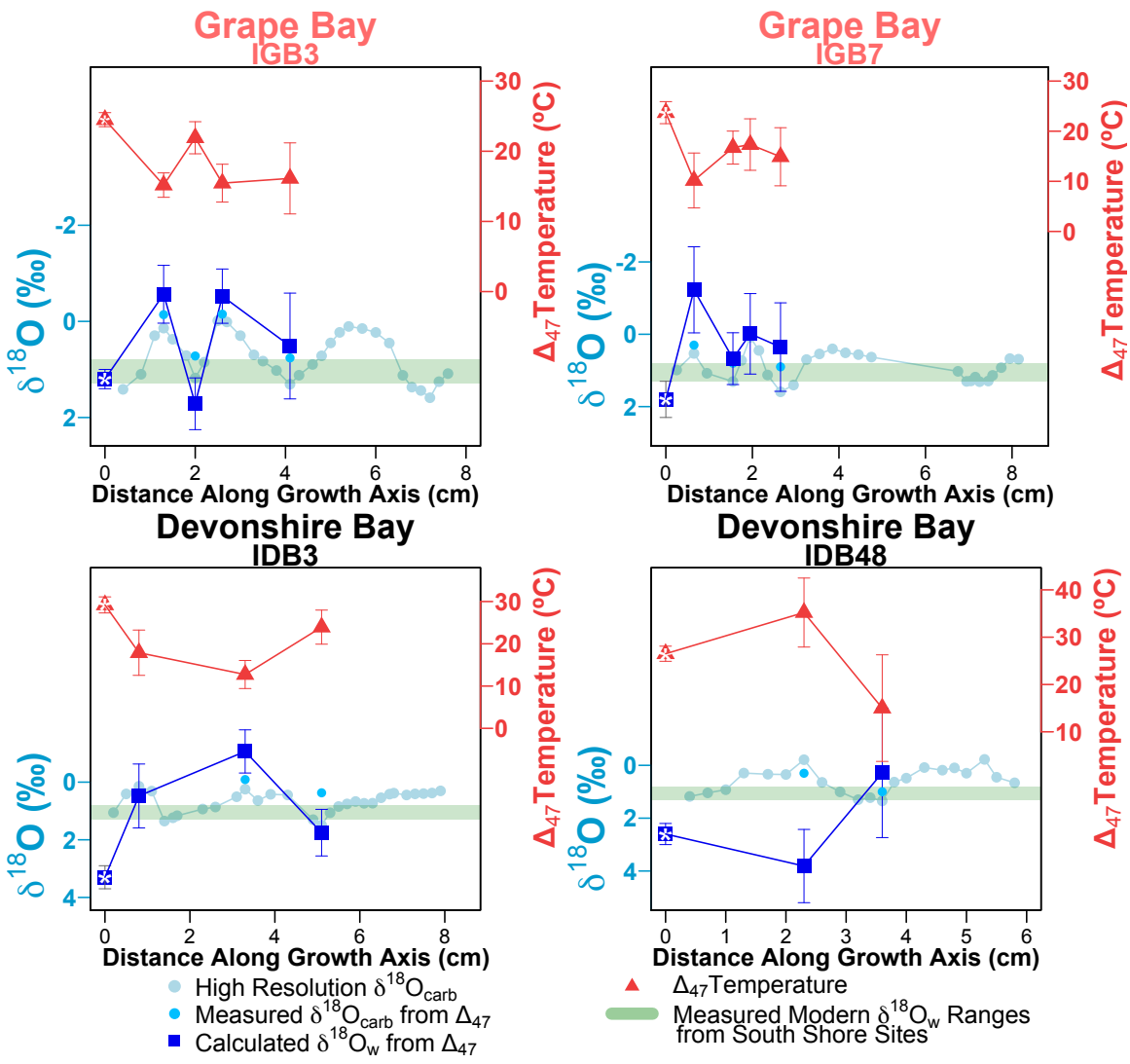

Figure S7. High resolution $\delta^{18}O$ measurements, Δ_{47}-based temperatures and $\delta^{18}O_w$ values, calculated using Kim et al., 2007 aragonite-water equilibrium equation, for four fossil shells. Note that the y-axes are scaled differently in each plot for best visibility of overlapping data.

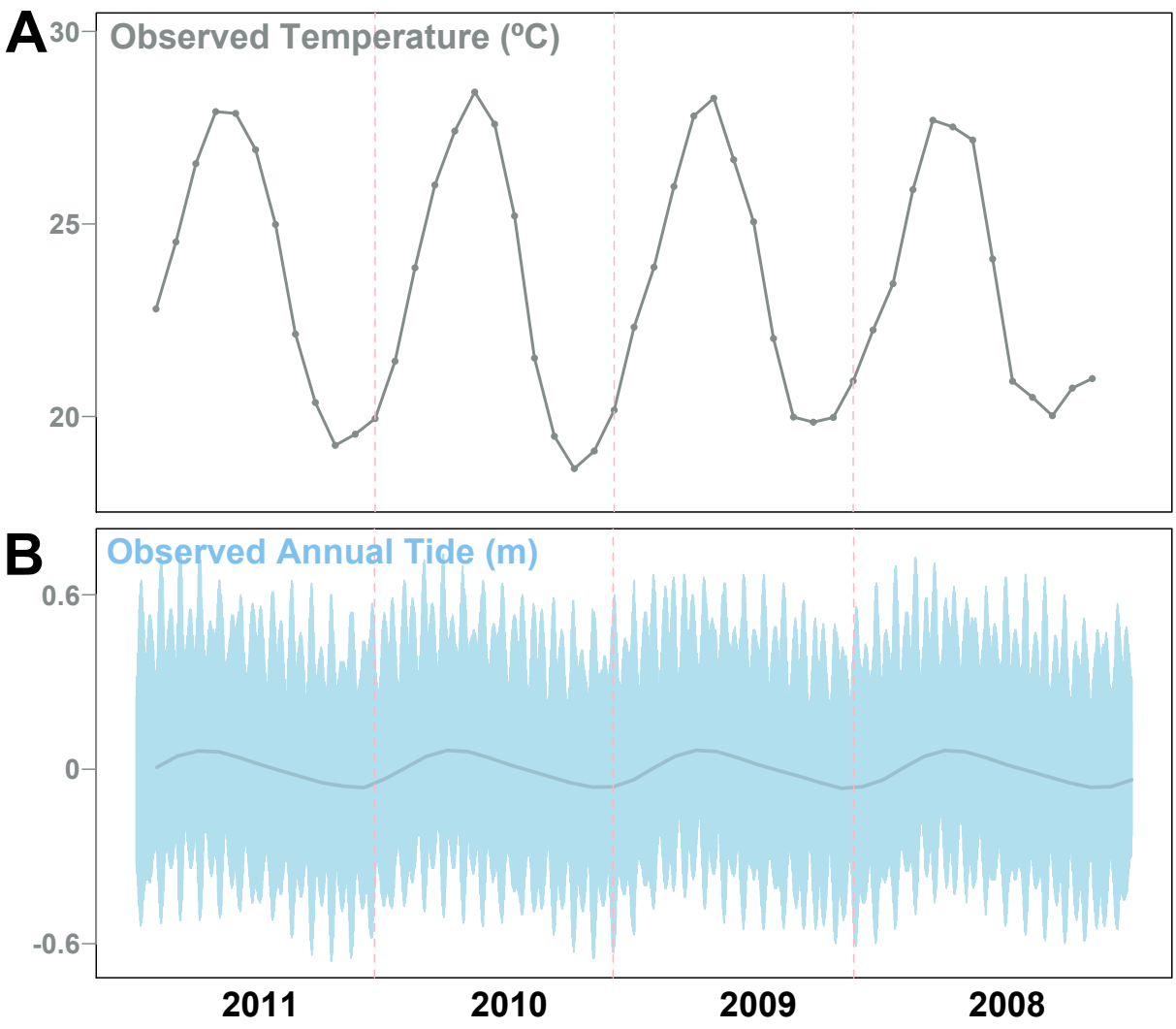

Figure S8. A, Observed modern (Instrumental) SST from 2008-2011 (NOAA National Data Buoy Center). B, Observed annual tide from 2008-2011 (NOAA Tides and Currents).

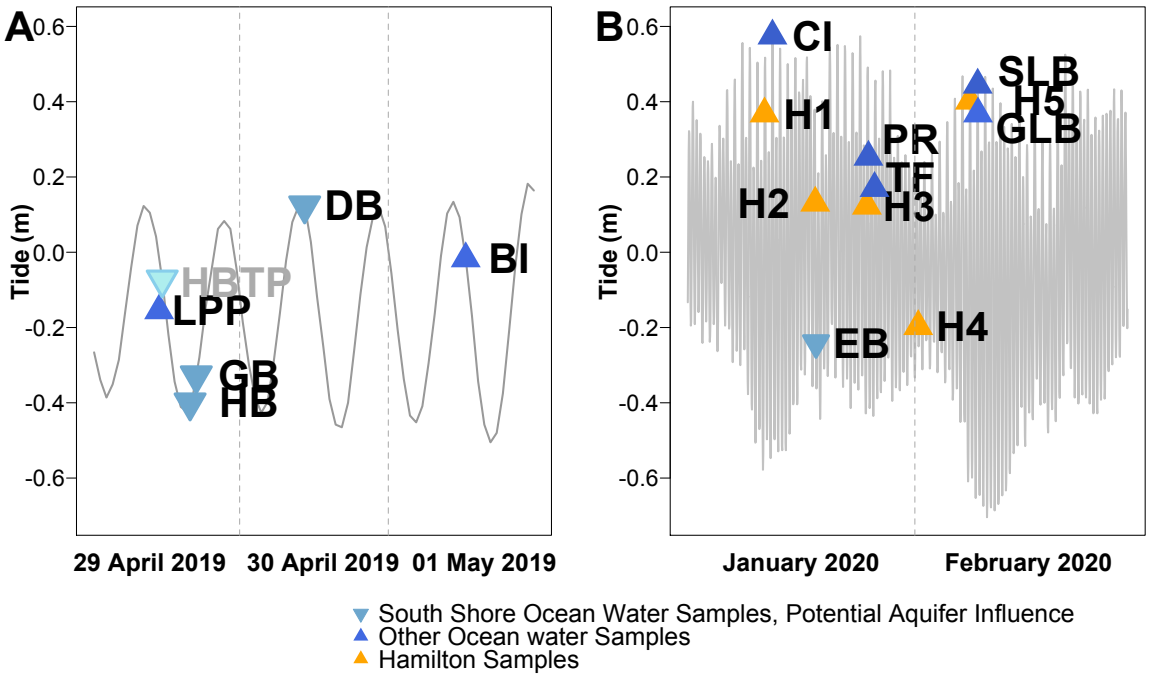

Figure S9. A, Tidal record during 2019 sampling period with each seawater sample plotted according to its collection time. Two letter labels identify collection site, as follows: BI=Bird Island; DB=Devonshire/Rocky Bay; GB=Grape Bay; LPP=Lodge Point Park; HB=Hungry Bay; and HBTP = stranded Tide Pool at Hungry Bay, plotted to represent tidal height of pool above seawater at time of collection. B, Tidal record during 2020 sampling period. Two letter labels identify collection site, as follows: CI=Cooper's Island; EB=Elbow Beach; GLB=Glass Beach; H1-5=Hamilton1-5; PR=Palmetto Roundabout; SLB=Somerset Long Bay, TF=The Flatts. Tide values are from NOAA Tides and Currents (https://tidesandcurrents.noaa.gov/).

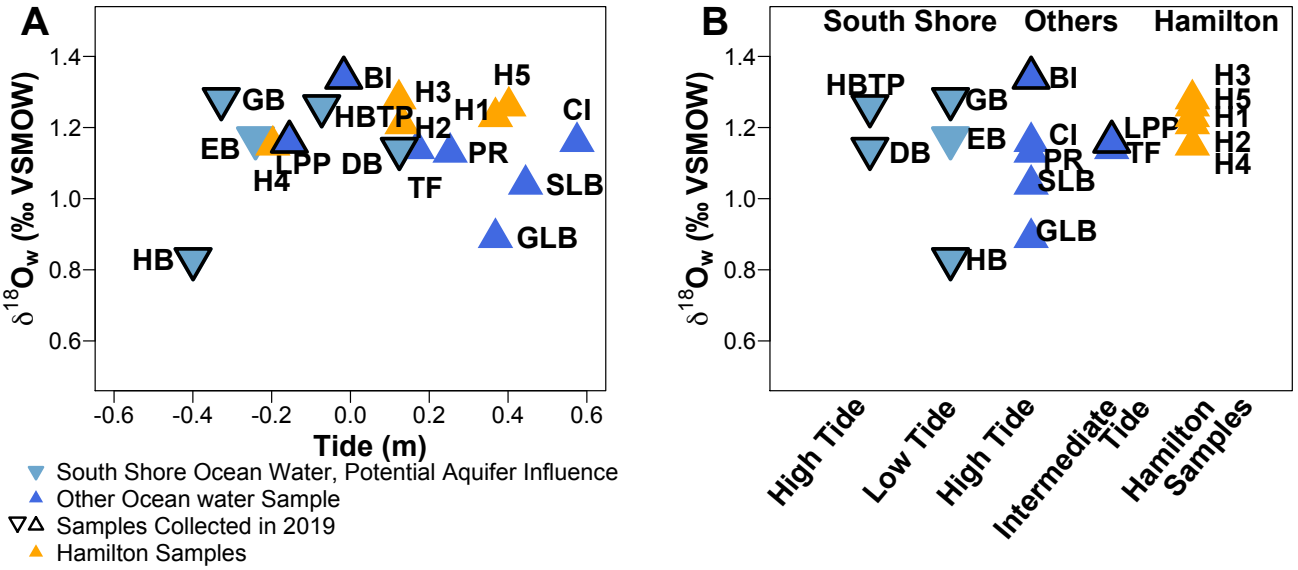

Figure S10. A, $\delta^{18}O_w$ values plotted against tidal height for all collected seawater samples. B, $\delta^{18}O_w$ values, with samples separated into tidal height categories (high/intermediate/low tide) and collection site (South Shore sites, non-South Shore sites, Hamilton). Two letter labels correspond to collection locality (see Table 1, Figure 6). Tide values are from NOAA Tides and Currents (https://tidesandcurrents.noaa.gov/).

Table S1. Salinity and isotope analyses data for each water sample